Scientific Research Publishing

Journal of High Energy Physics, Gravitation and Cosmology, 2026, 12(1), 252-266
https://www.scirp.org/journal/jhepgc
ISSN Online: 2380-4335
ISSN Print: 2380-4327

Graviton Redshift Theory of Dark Matter in Spiral and Dwarf Galaxies

Firmin J. Oliveira

East Asian Observatory/James Clerk Maxwell Submillimetre Telescope, Hilo, HI, USA
Email: firmjay@hotmail.com

How to cite this paper: Oliveira, F.J. (2026) Graviton Redshift Theory of Dark Matter in Spiral and Dwarf Galaxies. *Journal of High Energy Physics, Gravitation and Cosmology*, **12**, 252-266.
https://doi.org/10.4236/jhepgc.2026.121016

Received: October 23, 2025
Accepted: January 10, 2026
Published: January 13, 2026

Abstract

The theory that gravitons lose energy thru gravitational redshift while traveling against the force of a gravitational field is applied to spiral and dwarf galaxy rotation curves. A new coupling function for the graviton redshift energy is described which improves the predicting power of the theory. Fits are made to the rotation curves of both high and low surface brightness galaxies. Furthermore, for some of the galaxies, as a demonstration of the versatility of the theory, it is shown how adjustments to the mass profile velocities can reduce the error of the fit of the predicted to the observed rotation curve, thus giving feedback to the observing process. The energy of the gravitational redshift of gravitons is a viable candidate for dark matter in galaxies.

Keywords

Spiral Galaxies, Dark Matter, Gravitons, Gravitational Redshift, Baryon Mass Densities

1. Introduction

This paper describes a theory of gravitons acting in galaxies [1]. Assuming that gravitons are the agents of interaction in a gravitational field, then our goal is to describe how the gravitational redshift of gravitons caused by their traveling against the force of gravity shows up as what has traditionally been labeled as dark matter. We will show how the redshift of gravitons can explain this phenomenon of dark matter using high precision data. Only baryonic mass is required. We assume that gravitons are bosonic particles of zero rest mass which travel at constant speed c in vacuum, where the speed of gravity c equals the speed of light. The mass m associated with the graviton redshift energy is due to Einstein's mass to energy relation, $E = mc^2$, where E is the relativistic energy of the gravitons

which travel at speed c. Here, we will address only the gravitational energy loss (redshift energy) of the gravitons and not the full energy of the gravitons themselves.

Gravitons traveling in a gravitational field of a source baryonic mass M and a test mass m, modeled by the equivalence principle as an accelerating system, should experience an average energy loss of $\delta\xi$ by gravitational redshift due to motion against the force in that field, over a short time period $\delta t = \delta r/c$, where the acceleration a at a point r in the field is given by $a = -GM/r^2$. The energy loss is expressed differentially as,

$$\delta\xi = \left(m_g c^2\right)\frac{\delta v}{c} = \left(m_g c\right)a\delta t = -\left(\frac{GMm_g}{r^2}\right)\delta r, \tag{1}$$

where $m_g c^2 = mc^2/n$ is the average relativistically equivalent graviton mass energy, n is the number of gravitons, mc^2 is equal to the test mass rest energy, δv is the change in the free fall velocity of the system observed from an inertial reference frame, G is Newton's gravitational constant, M is the baryonic mass of the field source, r is the distance between the center of the source and the location of the moving gravitons, δt is the short travel time of the gravitons at speed c over distance δr.

Reiterating, the gravitons deliver a force given by Newton's law of gravitational force and in the delivery of this force, the gravitons themselves lose energy as they travel against the same gravitational force that they are delivering analogous to the energy loss of photons traveling away from the surface of a star. We call this effect of energy loss a gravitational redshift which means the average wavelength λ of the gravitons gets shifted towards the red end of the spectrum. It is completely consistent with General Relativity Theory [2].

2. Gravitons in Galaxies

Multiplying (1) by the number of gravitons n and integrating up to radial distance r we obtain the energy change of the gravitons $\Delta\Xi_g$ expressed proportionally by,

$$\Delta\Xi_g\left(r\right) \propto \int n\delta\xi = \int_0^v \left(nm_g c^2\right)\frac{\mathrm{d}u}{c} = -\int_0^r m\left(\frac{GM_b\left(u\right)}{u^2}\right)\mathrm{d}u, \tag{2}$$

where we substituted $m = nm_g$ in the final result. Equation (2) describes the gravitational redshift of the energy of the gravitons as they travel from a lower, more negative potential to a position r of higher, less negative potential and is consistent with energy conservation.

Now, consider the energy of a small mass m in a circular orbit of radius r in a galaxy of baryonic mass $M_b\left(r\right)$ interior to m. The gravitons which traverse the distance at lightspeed from the interior mass to deliver the attractive force to the orbiting mass will experience a decrease in energy as described by (2), which is essentially a form of potential energy $m\phi_g\left(r\right)$ due to the redshift of the gravitons, expressed by,

$$m\phi_g(r)=\Delta\Xi_g(r)=-mK(r)\int_0^r\left(\frac{GM_b(u)}{u^2}\right)\mathrm{d}u, \tag{3}$$

where $K(r)$ is a coupling factor. We hypothesize that the coupling factor $K(r)$ has the form,

$$K(r)=k\left(\frac{r_f}{r}\right)^{\beta}\left(\frac{M_b(r)}{M_{bgal}}\right), \tag{4}$$

where k and β are coupling constants, r_f is the observed final radial position and $M_{bgal}=M_b(r_f)$ is the galaxy total baryonic mass.

We utilize the virial theorem for a gravitational system in equilibrium possessing kinetic energy KE and potential energy $m\phi(r)$, where $KE=-(1/2)m\phi(r)$, where the potential energy is the sum of the Newtonian potential energy $m\phi_N(r)=-mGM_b(r)/r$ and the potential energy $m\phi_g(r)$ due to the graviton energy loss. Taking the graviton energy loss into account, using (3) and (4), and the Newtonian potential energy, we express the total kinetic energy of the orbiting mass m by,

$$\begin{aligned}\frac{1}{2}mv^2&=-\frac{1}{2}m\left(\phi_N(r)+\phi_g(r)\right)\\&=-\frac{1}{2}\left(-\frac{mGM_b(r)}{r}-k\left(\frac{r_f}{r}\right)^{\beta}\left(\frac{M_b(r)}{M_{bgal}}\right)\int_0^r\left(\frac{mGM_b(u)}{u^2}\right)\mathrm{d}u\right),\end{aligned} \tag{5}$$

where v is the rotational velocity of the orbiting mass m. Simplifying (5) we obtain the expression for the orbital velocity,

$$v^2=-\phi(r)=\frac{GM(r)}{r}, \tag{6}$$

where the total potential $\Phi(r)$ is defined by,

$$\phi(r)=\phi_N(r)+\phi_g(r). \tag{7}$$

and the mass function $M(r)$ is defined by,

$$M(r)=M_b(r)\left(1+\left(\frac{kr}{M_{bgal}}\right)\left(\frac{r_f}{r}\right)^{\beta}\int_0^r\left(\frac{M_b(u)}{u^2}\right)\mathrm{d}u\right). \tag{8}$$

The coupling constant k can be determined at the final radial position r_f and final rotation velocity v_f, given by,

$$k=\frac{\left(v_f^2-\dfrac{GM_{bgal}}{r_f}\right)}{\left(\displaystyle\int_0^{r_f}\left(\frac{GM_b(u)}{u^2}\right)\mathrm{d}u\right)}. \tag{9}$$

With the value obtained for k then the constant β can be determined by minimizing the error of the fit of the predicted rotation curve (6-8), $v^2(r)$, to the observed rotation curve, $v_{obs}^2(r)$.

3. Results

We use the velocities from the Spitzer Photometry and Accurate Rotation Curves (SPARC) data base [3] [4], derived from near-infrared (NIR) surface photometry at 3.6 μm. We select the spiral galaxies NGC 2903, NGC 6503, NGC 7814, DDO 154, UGC A442 and NGC 6674. Only two galaxies have bulges (NGC 7814 and NGC 6674). From the photometric data which has been reduced to the equivalent velocities for the galaxy bulge, disk and gas mass content, we calculate the baryonic mass function $M_b(r)$ within radial distance r from the galaxy center as due to a spherically symmetric distribution using the Newtonian relation,

$$M_b(r)=\left(\frac{r}{G}\right)\left(\left(\left|v_{gas}(r)\right|v_{gas}(r)\right)+\Upsilon_{dsk}\left(\left|v_{dsk}(r)\right|v_{dsk}(r)\right)+\Upsilon_{bul}\left(\left|v_{bul}(r)\right|v_{bul}(r)\right)\right), \tag{10}$$

where $r=r_k$, $k=1,2,\cdots,N$, $N>1$, N the number of radial distances observed, and the absolute values of the velocities are needed because they can sometimes be negative ([4]: p. 5). To simplify the analysis, we set the mass to light ratios for the disk and bulge equal, $\Upsilon_{dsk}=\Upsilon_{bul}=\Upsilon_*$. The rotation curve observed velocities and the mass profile velocities for the disk, bulge and gas are taken from [3]. To obtain a realistic baryonic mass profile $M_b(r)$ using (10), a pseudo model $M_{bx}(r)$ for the baryonic mass is utilized, which is taken in the form,

$$M_{bx}(r)=\frac{v^2(r)}{(G/r)\left(1+\left(r/r_b(r)\right)\right)}, \tag{11}$$

where $r_b(r)$ is defined by,

$$r_b(r)=\left(\frac{r_{b0}}{r_{bx}(r_f)}\right)r_{bx}(r), \tag{12}$$

where r_{b0} is defined at the final rotation point (v_f,r_f),

$$r_{b0}=\frac{GM_{bgal}}{v_f^2-\left(GM_{bgal}/r_f\right)}, \tag{13}$$

and $r_{bx}(r)$ is defined,

$$r_{bx}(r)=\frac{GM_b(r)}{v^2(r)-\left(GM_b(r)/r\right)}. \tag{14}$$

This definition ensures that the final value $r_b(r_f)=r_{b0}$ and that $r_b(r)$ approaches $r_{bx}(r)$ as the iteration progresses. Thus, we iterate on Υ_* in (10) until $M_b(r)=M_{bx}(r)$ is in close approximation. Using the SPARC results at radial distance r for the gas, disk and bulge velocities for the galaxy, where the mass internal to r is given by $M_b(r)$ of (10), we obtain the equivalent graviton energy loss using (3) and (4), where the graviton mass function $M_g(r)=-PE_g(r)(r/G)$, giving us the relation,

$$M_g(r_n) = k\left(\frac{r_f}{r_n}\right)^{\beta}\left(\frac{M_b(r_n)}{M_{bgal}}\right)\left(\frac{r_n}{G}\right)\sum_{j=1}^{n}\left(\int_{r_{j-(j>1)}}^{r_j}\left(\frac{GM_b(u)}{u^2}\right)\mathrm{d}u\right). \quad (15)$$

The predicted velocity (6) using (10) and (15) is expressed in the form,

$$v^2(r_j) = \frac{G\left(M_b(r_j) + M_g(r_j)\right)}{r_j}, \quad (16)$$

where $j = 1, 2, \cdots, N$, $N > 1$. For clarity, in (15) the logical expression term $(j > 1)$ equals 1 if j is greater than 1, and zero otherwise.

Table 1 shows data used for the galaxy fits. The baryonic mass for each galaxy fit is the result of iterating on the mass to light ratio Υ_* in (10) until the final Newtonian velocity due to the total baryonic mass closely equals the SPARC data analysis result from the photometry. The relation of the fitted baryonic mass M_{bgal} to the Baryonic Tully-Fisher Relation (BTFR) mass for the galaxy [5] [6] is given as a ratio, with $M_{btfr} = 50v_f^4$, where v_f is simply the final measured velocity of the galaxy (rather than a smooth average of the end of the rotation curve). The distance to each galaxy in megaparsecs is also given.

Table 1. Results of fits to SPARC galaxy data for the galaxies shown using the graviton model (6-8) with total baryonic mass M_{bgal} from (10). The distance to each galaxy is shown, along with the final velocity v_f and radial position r_f used in making the fits. The total dark matter mass M_{ggal} is shown, which is the total equivalent relativistic graviton redshift mass from (15).

Galaxy	M_{bgal}	Distance	v_f	r_f	M_{bgal}/M_{btfr}	M_{ggal}
	($M_\odot \times 10^{10}$)	(Mpc)	(km·s^{-1})	(kpc)		($M_\odot \times 10^{10}$)
NGC 2903	3.989	6.6	180	24.96	0.76	14.705
NGC 6503	1.093	6.26	115	23.5	1.25	6.129
NGC 7814	5.2432	14.4	214	19.53	0.500	15.547
DDO 154	0.03643	4.04	45.5	5.92	1.700	0.249
UGC A442	0.04841	4.35	56.5	6.33	0.950	0.421
NGC 6674	16.634	51.2	242	72.41	0.970	81.946
NGC 3198	3.894	13.8	149	44.08	1.580	18.902

We remark that there are two galaxies, UGC A442 and NGC 6674, which have total galaxy baryonic masses M_{bgal} approximating the M_{btfr} mass specified above, with a normalization of 50 and an exponent of 4, at 95% and 97% respectively [5] and [6]. For the other four galaxies an exponent of 4.0001 predicts the determined baryonic masses. For the six galaxies overall we obtain a scatter for M_{bgal}/M_{btfr} of $\sigma = 0.074$ dex which is within the intrinsic scatter of $\sigma_{int} \approx 0.11$ dex for the BTFR study in [6].

Table 2 gives the mass to light ratio Υ_* for the disk and bulge combined. The coupling parameters k and β are given. A positive value for β implies a dependence proportional to $1/r$, while a negative value for β implies a dependence proportional to r. The fitting error is computed as the mean absolute error

of the squared velocities, $\langle \text{FitErr} \rangle = \sqrt{(1/N)\sum_{j=1}^{N}\left(\left\| v^2(r_j) - v_{obs}^2(r_j)\right\|\right)}$. The average mass to light ratio for the 6 galaxies is $\langle \Upsilon_* \rangle = 0.528\ \mathrm{M}_\odot/\mathrm{L}_\odot$ which is agreeable with the realistic value $0.5\ \mathrm{M}_\odot/\mathrm{L}_\odot$ for galaxies found in [4].

Table 2. Results of fits to SPARC galaxy data using the graviton model (6-8). Υ_* is the same for disk and bulge components. Also shown are the derived coupling constants k and β for each galaxy. $\langle \text{FitErr} \rangle$ is the average of the absolute value of the differences of the predicted and observed squared velocities.

Galaxy	Υ_*	k	β	$\langle \text{FitErr} \rangle$
	($\mathrm{M}_\odot/\mathrm{L}_\odot$)			(km/s)
NGC 2903	0.414	0.2785	0.009	47.643
NGC 6503	0.568	0.4905	0.136	22.315
NGC 7814	0.645	0.2123	−0.279	39.502
DDO 154	0.513	3.1309	1.201	5.561
UGC A442	0.430	1.7909	−0.188	6.508
NGC 6674	0.598	0.318	−0.017	15.888
NGC 3198	0.400	0.8575	0.785	33.587

Figure 1 shows the galaxy rotation curves. The galaxies in the top row, NGC 2903, NGC 6503 and NGC 7814 have fits made with variations to mass to light ratio Υ_*, coupling constant k and coupling exponent β, but no adjustments to the photometric mass definition. The galaxies in the bottom row have fits made with variations to mass to light ratio Υ_*, coupling constant k and coupling exponent β plus, as well, adjustments were made to the bulge and gas velocities in the photometric definition (15). For the bottom row, galaxies DDO 154 and UGC A442 have their gas velocities adjusted in the photometric definition to make a better fit to their rotation curves. Galaxy NGC 6674 has adjustments to both bulge and gas velocities of its photometric definition to improve the fit.

In both top and bottom plots, using only the SPARC data, the solid magenta line is for the disk and bulge velocity mass profiles. The solid green line is for the gas velocity mass profile. The solid blue line is for the sum of the disk, bulge and gas velocity mass profiles, which is the Newtonian velocity due to the baryonic mass profile. The solid red line with open circles is for the graviton redshift (dark matter) velocity. The simple solid red line is the sum of the Newtonian and graviton redshift (dark matter) velocities. The dashed black line with open circles and error bars is the SPARC velocity and error data values.

In the bottom plots, where we made adjustments to the SPARC data, the dashed magenta line is the adjusted bulge (and disk) velocity mass profile. The dashed green line is the adjusted gas velocity mass profile. The dashed red line with open

circles is the graviton redshift (dark matter) velocity result due to the adjustments to the mass profiles. The simple dashed red line is the sum of the Newtonian and graviton redshift (dark matter) velocities result due to the adjustments to the mass profiles.

4. Modeling a Galaxy by a Star Interior

We sketch how the GRST for galaxies can be treated similar to the interior of a star defined in terms of General Relativity. In this section only, we set $G = c = 1$ to simplify the equations. The metric tensor for a spherically symmetric system in a coordinate system (t, r, θ, ϕ) is static (not dependent on time t) and defined,

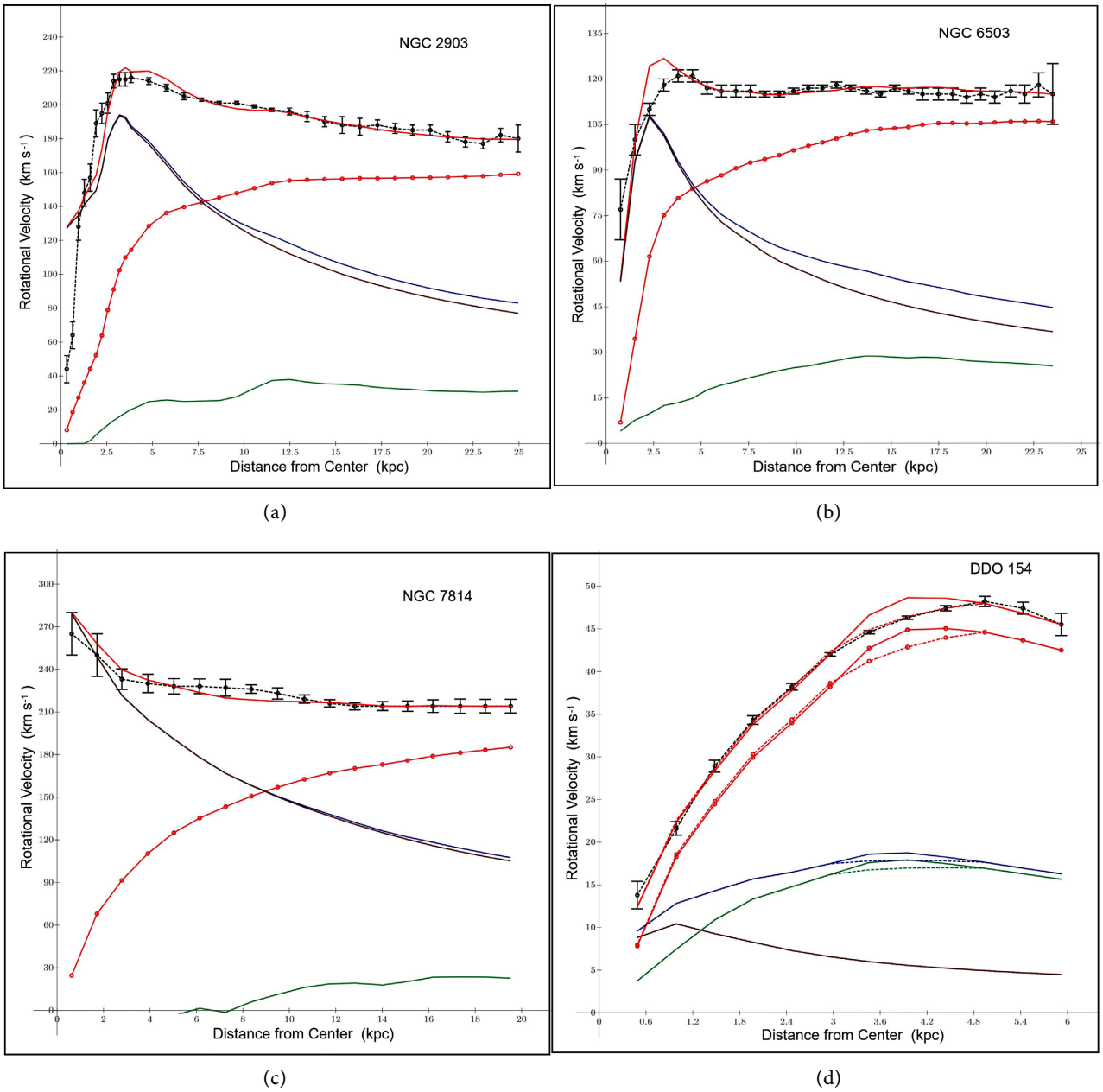

(a) (b)

(c) (d)

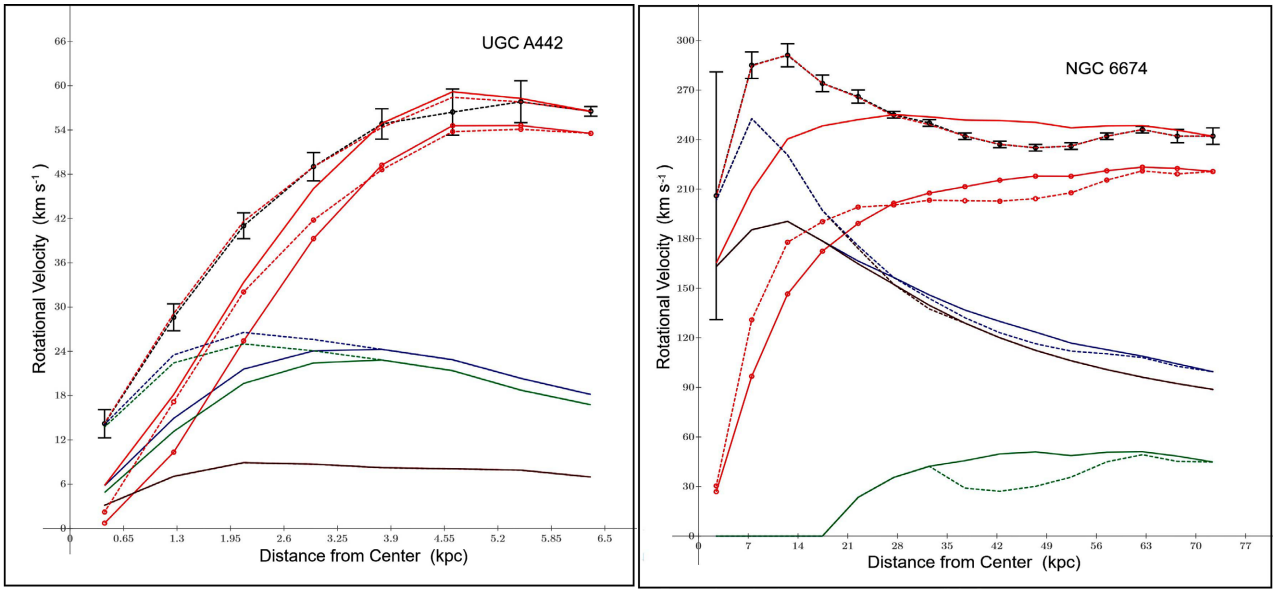

(e) (f)

Figure 1. Fits with SPARC data, the masses $M_b(r)$ and $M_g(r)$ derived from (10) and (15), respectively, with velocity profiles for gas, disk and bulge. In the top row, NGC 2903, NGC 6503 and NGC 7814 have no adjustments. In the bottom row, DDO 154, UGCA442 and NGC6674 have adjustments to gas velocity and for NGC 6674 there is also adjustment to the disk velocity. In both top and bottom plots, the solid magenta line is for the disk and bulge velocity mass profiles. The solid green line is for the gas velocity mass profile. The solid blue line is for the sum of the disk, bulge and gas velocity mass profiles, which is the Newtonian velocity due to the baryonic mass profile. The solid red line with open circles is for the graviton redshift (dark matter) velocity. The plain solid red line is the sum of the Newtonian and graviton redshift (dark matter) velocities. The dashed black line with open circles and error bars are the SPARC velocity and error data values. In the bottom plots the dashed magenta line is the adjusted bulge and disk velocity mass profile, where only the bulge profile was adjusted. The dashed green line is the adjusted gas velocity mass profile. The dashed red line with open circles is the result for the graviton redshift (dark matter) velocity due to the adjustments to the mass profiles. The plain dashed red line is the sum of the Newtonian and graviton redshift (dark matter) velocities due to the adjustments to the mass profiles.

$$\mathrm{d}s^2 = -\mathrm{e}^{2\Phi}\mathrm{d}t^2 + \mathrm{e}^{2\Lambda}\mathrm{d}r^2 + r^2\mathrm{d}\theta^2 + r^2\sin^2(\theta)\mathrm{d}\phi^2, \tag{17}$$

where $\Phi = \Phi(r)$ and $\Lambda = \Lambda(r)$ are functions of r only. Inside of a galaxy in equillibrium, with an entropy $\epsilon \approx \text{constant}$, with pressure p and density ρ both non-zero, we assume that an equation of state exists such that the pressure is a function of the density, $p(r) = p(\rho(r))$. We substitute $m(r)$ which is a function of r only, for $\Lambda(r)$ without loss of generality, by the form [7],

$$m(r) = \left(\frac{r}{2}\right)\left(1 - \mathrm{e}^{-2\Lambda(r)}\right), \tag{18}$$

giving us upon inversion,

$$\mathrm{e}^{2\Lambda(r)} = \left(1 - \frac{2m(r)}{r}\right)^{-1}. \tag{19}$$

We call $m(r)$ the mass function rather than the energy mass. More specifically, $m(r)$ represents the baryonic mass.

Consider the Einstein field equation $G_{\mu\nu} = 8\pi T_{\mu\nu}$, where $\mu,\nu \in (t,r,\theta,\phi)$.

The $(0,0)$ and (r,r) components of the field equation are given by,

$$\begin{aligned} G_{00} &= \frac{1}{r^2}\mathrm{e}^{2\Phi}\frac{\mathrm{d}}{\mathrm{d}r}\left[r\left(1-\mathrm{e}^{-2\Lambda}\right)\right] = \rho\mathrm{e}^{2\Phi}, \\ G_{rr} &= -\frac{1}{r^2}\mathrm{e}^{2\Lambda}\left(1-\mathrm{e}^{-2\Lambda}\right)+\frac{2}{r}\frac{\mathrm{d}\Phi}{\mathrm{d}r} = p\mathrm{e}^{2\Lambda}. \end{aligned} \tag{20}$$

The G_{00} equation in (20) simplifies to,

$$\frac{\mathrm{d}}{\mathrm{d}r}\left[r\left(1-\mathrm{e}^{-2\Lambda}\right)\right] = \rho r^2. \tag{21}$$

Integrating (21) and using (18) for $m(r)$ yields,

$$m(r) = \int \mathrm{d}\left[r\left(1-\mathrm{e}^{-2\Lambda}\right)\right] = \int_0^r 4\pi r^2\rho(r)\mathrm{d}r. \tag{22}$$

We get $\Phi(r)$ from the G_{rr} equation of (20). Solving for $\mathrm{d}\Phi/\mathrm{d}r$ gives,

$$\frac{\mathrm{d}\Phi(r)}{\mathrm{d}r} = \frac{m(r)+4\pi r^3 p}{r\left(r-2m(r)\right)}. \tag{23}$$

The equation of motion can be obtained from (17) by dividing it by $\mathrm{d}\tau^2/\mu^2$, where $\mathrm{d}\tau$ is the interval of proper time and μ is the rest mass of the system [8]. We have,

$$-\mu^2 = \mu^2\frac{\mathrm{d}s^2}{\mathrm{d}\tau^2} = \mu^2\left(-\left(\mathrm{e}^{2\Phi(r)}\right)\frac{\mathrm{d}t^2}{\mathrm{d}\tau^2}+\left(\mathrm{e}^{2\Lambda(r)}\right)\frac{\mathrm{d}r^2}{\mathrm{d}\tau^2}+r^2\frac{\mathrm{d}\theta^2}{\mathrm{d}\tau^2}+r^2\sin^2(\theta)\frac{\mathrm{d}\phi^2}{\mathrm{d}\tau^2}\right). \tag{24}$$

For motion in the plane, assume $\theta=\pi/2$, $\mathrm{d}\theta=0$ so that $\sin(\theta)=1$. Since $\mathrm{d}t/\mathrm{d}\tau = E/\mathrm{e}^{2\Phi(r)}$ and $\mathrm{d}\phi/\mathrm{d}\tau = L/r^2$, where E is the energy and L is the angular momentum, we manipulate (24) to get the form,

$$\frac{-1}{\mathrm{e}^{2\Lambda(r)}} = -\frac{\tilde{E}^2}{\left(\mathrm{e}^{2\Phi(r)}\right)\left(\mathrm{e}^{2\Lambda(r)}\right)}+\frac{\mathrm{d}r^2}{\mathrm{d}\tau^2}+\frac{\tilde{L}^2}{r^2\left(\mathrm{e}^{2\Lambda(r)}\right)}, \tag{25}$$

where the energy per unit mass $\tilde{E}=E/\mu$ and the angular momentum per unit mass $\tilde{L}=L/\mu$.

Assume $\Phi(r)=-\Lambda(r)-\Omega(r)$ for some function $\Omega(r)$. This implies that,

$$2\left(\Phi(r)+\Lambda(r)\right) = 2\left(-\Lambda(r)-\Omega(r)+\Lambda(r)\right) = -2\Omega(r). \tag{26}$$

Substituting from (26) into (25) and rearranging it into the standard form yields,

$$\frac{\mathrm{d}r^2}{\mathrm{d}\tau^2} = \tilde{E}^2\mathrm{e}^{2\Omega(r)}-\frac{1}{\mathrm{e}^{2\Lambda(r)}}\left(\frac{\tilde{L}^2}{r^2}+1\right). \tag{27}$$

Define $\mathrm{e}^{2\Omega(r)}$ with reference to (3) and (4),

$$\mathrm{e}^{2\Omega(r)} = 1+\left(\tilde{E}^{-2}\right)K(r)\int_0^r\left(\frac{m(u)}{u^2}\right)\mathrm{d}u, \tag{28}$$

where coupling function $K(r)=k\left(r_f/r\right)^{\beta}\left(m(r)/m(r_f)\right)$, where k and β are coupling constants and $m(r_f)$ is the total galaxy baryonic mass within radius r_f. With (28) substituted into (27) and substituting from (19) for $\mathrm{e}^{2\Lambda(r)}$ we obtain,

$$\frac{\mathrm{d}r^2}{\mathrm{d}\tau^2}=\tilde{E}^2+K(r)\int_0^r\left(\frac{m(u)}{u^2}\right)\mathrm{d}u-\left(1-\frac{2m(r)}{r}\right)\left(\frac{\tilde{L}^2}{r^2}+1\right). \tag{29}$$

Equation (29) is equivalent to the GRST energy equation in (6) along with (8). We obtain $\Phi(r)$ from the G_{rr} equation of (20). Solving for $\mathrm{d}\Phi/\mathrm{d}r$ gives,

$$\frac{\mathrm{d}\Phi(r)}{\mathrm{d}r}=\frac{m(r)+4\pi r^3p}{r(r-2m(r))}=-\frac{\mathrm{d}}{\mathrm{d}r}(\Lambda(r)+\Omega(r)), \tag{30}$$

where, using (19) and (28) we have for $\Lambda(r)$ and $\Omega(r)$, respectively,

$$\begin{aligned}\Lambda(r)&=\frac{1}{2}\ln\left(\frac{1}{1-2m(r)/r}\right)=-\frac{1}{2}\ln\left(1-\frac{2m(r)}{r}\right),\\ \Omega(r)&=\frac{1}{2}\ln\left(1+\left(\tilde{E}^{-2}\right)K(r)\int_0^r\left(\frac{m(u)}{u^2}\right)\mathrm{d}u\right).\end{aligned} \tag{31}$$

The pressure p can be obtained from (30) and (31),

$$p=-\left(\frac{\rho(r)}{3}\right)-\left(\frac{r(r-2m(r))}{4\pi r^3}\right)\frac{\mathrm{d}}{\mathrm{d}r}\left(\frac{1}{2}\ln\left(\frac{1+\left(\tilde{E}^{-2}\right)K(r)\int_0^r\left(m(u)/u^2\right)\mathrm{d}u}{1-2m(r)/r}\right)\right), \tag{32}$$

where density $\rho(r)=m(r)/(4\pi/3)r^3$.

Beyond the boundary edge of the galaxy, $r\geq r_f$, where the density and pressure $\rho=p=0$, the $(0,0)$ and (r,r) components of the external metric tensor $g_{ext,\mu\nu}$ for the galaxy are given by the Schwarzschild metric,

$$\begin{aligned}g_{ext,00}(r)&=1-\frac{2M}{r},r\geq r_f,\\ g_{ext,11}(r)&=\left(1-\frac{2M}{r}\right)^{-1},r\geq r_f,\end{aligned} \tag{33}$$

where the total galaxy mass M of baryonic plus graviton redshift energy loss (dark matter) is given by,

$$M=m(r_f)+r_fk\int_0^{r_f}\left(\frac{m(u)}{u^2}\right)\mathrm{d}u. \tag{34}$$

The dynamical equations are identical for the rotational motion beyond the boundary $r\geq r_f$ for the internal and external velocities in the Newtonian approximation,

$$v^2(r)=\frac{m(r_f)+r_fk\int_0^{r_f}\left(\frac{m(u)}{u^2}\right)\mathrm{d}u}{r}=v_{ext}^2(r_f)=\frac{M}{r}. \tag{35}$$

5. Discussion

We look at a couple of dark matter papers and a paper on graviton detection. In [9] is a quantum graviton-graviton interaction theory of gravity in which a potential is theoretically derived having the form,

$$V(r)=-GM(r)\left(\frac{1}{r}-\frac{b}{2\pi a}\ln\left(r/r_c\right)\right), \tag{36}$$

where $a=GM\tau$ where τ is a dimensionless proportionality constant, the squared velocity parameter $b=b_0+b_1\sqrt{GM/c^2R}+b_2\left(GM/c^2R\right)+\cdots$, where M is the total galaxy mass, the b_n are squared velocity constants with $b_0=0$ and r_c is an initial radial distance. Assuming R is large enough so that $\sqrt{GM/c^2R}\gg\left(GM/c^2R\right)$, this implies that $b\approx b_1\sqrt{GM/c^2R}$. Then, equating (36) with our potential in (6), and simplifying yields the relation for the dark matter energy connecting both methods,

$$k\left(\frac{r_f}{r}\right)^{\beta}\left(\frac{M(r)}{M_{bgal}}\right)\int_0^r\frac{GM(u)}{u^2}\mathrm{d}u=\left(\frac{b_1}{2\pi\tau}\sqrt{GM_{bgal}/c^2R}\right)\ln\left(r/r_c\right). \tag{37}$$

In Figure 2, we show a plot of the rotation curves for NGC 3198 which is also analyzed in [9]. The curves have the same legends as for rotation curves shown in Figure 1. The two extra light blue curves are for the quantum gravity velocity prediction potential (36). The dashed light blue line is the graviton-graviton interaction due to the second term in the potential (dark matter). The solid light blue line is the predicted velocity of (36), which is the sum of the Newtonian and graviton-graviton interaction velocities. The parameters for the fit are length $\tau=0.006$, $b_1=1500\ \mathrm{km^2\cdot s^{-2}}$, $R=330GM_{bgal}/c^2$ where $M_{bgal}=3.894\times10^{10}\ \mathrm{M_\odot}$ is the total baryonic mass of NGC 3198, $r_c=8$ pc. Although the fit is not dramatic due in part to the fact that the theoretical baryonic mass distribution in [9] is based on an exponential density $\rho(r)=M\mathrm{e}^{-r/r_0}$ whilst the luminosity profile from SPARC which we used to determine the mass distribution is likely not an exponential function. This may explain the poor fit.

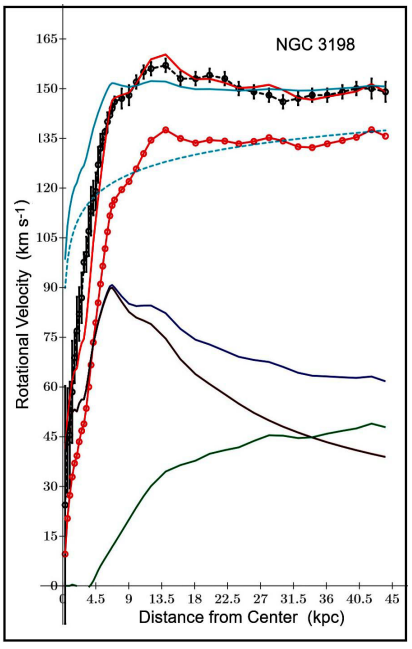

(a)

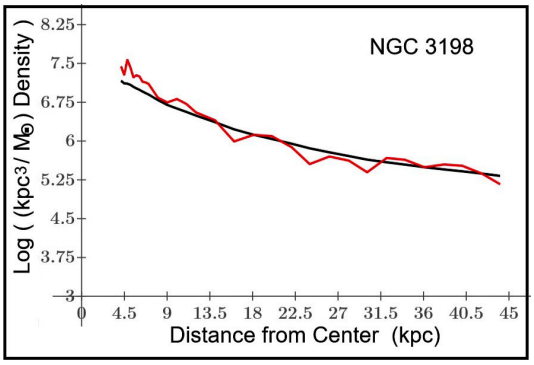

(b)

Figure 2. Fits with SPARC velocity data for NGC 3198, the masses $M_b(r)$ and $M_g(r)$ derived from (10) and (15), respectively, where in the top plot are the velocity profiles for gas, disk and bulge and in the bottom plot are the mass densities $\rho(r)$ and $\rho_m(r)$ from (40) and (41), respectively. In the top plot the solid magenta line is for the disk and bulge mass velocity profiles. The solid green line is the gas mass velocity profile. The solid blue line is the sum of the disk, bulge and gas velocity profiles which forms the Newtonian velocity profile. The solid red line with open circles is the graviton redshift (dark matter) velocity. The plain solid red line is the sum of Newtonian and graviton redshift velocities. The dashed black line with open circles and error bars are the SPARC velocity and error data values. The dashed light blue line is the dark matter velocity of the graviton-graviton interaction theory, second term on right hand side of (36). The solid light blue line is the total predicted rotation velocity for the graviton-graviton interaction theory (36).

In the paper [10], the study is made of the density of dark matter in the external regions of the galaxy rotation curve, beyond the presumed critical radius r_c of the baryonic particles. (However, in NGC 3198 the baryons likely extend throughout the entire galaxy.) The basic equation that is used to determine the mass in the galaxy is the following,

$$\int_0^r 4\pi s^2 \rho(u)\,\mathrm{d}u = \frac{rv^2(r)}{G}. \tag{38}$$

Taking a step back, since the rotation curve velocity is only one of the three possible components, the radial component v_r deduced from the measured radial velocity of the galaxy, its value should be multiplied by $\sqrt{3}$ to obtain a better estimate of the true velocity. Taking the derivative of (38) with respect to r, and accounting for the multiple of $\sqrt{3}$ on $v(r)$, gives the expression,

$$\frac{\mathrm{d}}{\mathrm{d}r}\left(\int_0^r 4\pi u^2 \rho(u)\,\mathrm{d}u\right) = 4\pi r^2 \rho((r) = \frac{\mathrm{d}}{\mathrm{d}r}\left(\frac{3rv^2(r)}{G}\right). \tag{39}$$

Therefore, the density in (39) is given by,

$$\rho(r) = \left(\frac{3}{4\pi G r^2}\right)\frac{\mathrm{d}}{\mathrm{d}r}\left(\frac{rv^2(r)}{G}\right), \tag{40}$$

which is a multiple of 3 compared to ([10], Equation (5)) If we define a density $\rho_m(r)$ in terms of the mass function $M(r)$ for the baryonic mass $M_b(r)$ and

dark matter mass $M_g(r)$, $M(r)=M_b(r)+M_g(r)$, then we have,

$$\rho_m(r)=\frac{M_b(r)+M_g(r)}{(4\pi/3)r^3}. \tag{41}$$

Figure 2 shows a plot of $\log(\rho(r))$ and $\log(\rho_m(r))$ for galaxy NGC 3198, which are in reasonable agreement. This supports our argument regarding the factor $\sqrt{3}$ made above. Comparing with [10] we notice that multiplying the density by 3, that is $3\rho_{dm}(r)$, makes the start of the $\log(\rho_{dm}(r_c=4.5\text{ kpc}))$ approximately $\log(3)+3.3\approx 3.8$ on the log scale, where our starting value at 4.5 kpc is about 7.5 on the log scale. In summary, Table 1 and Table 2 show the parameters and fit values for NGC 3198.

In a third paper, it is theorized that if a large detector the size of the planet Jupiter is placed in orbit near a neutron star under ideal conditions (no background noise sources), then only one graviton would be detected in 10 years [11]. By contrast, the massiveness of a galaxy may be what enables the detection of the gravitons by the orbiting star or gas. Extrapolating linearly, the mass of a dwarf galaxy is about $10^8\,M_\odot$ which equals about 10^{11} Jupiters, which implies that 10^{10} gravitons can be detected per year or about 3 gravitons per second. Therefore, a star or gas in a galactic orbit should be succeptible to the flux of gravitons from the galaxy.

The energy of the gravitational redshift of gravitons fulfills all the requirements attributed to dark matter: it does not radiate light and it does not interact by any other means except thru gravity.

6. Conclusions

We have presented the graviton redshift theory (GRST) previously in [12] [13]. However, in the present form, the theory more strongly behaves as a function of the baryonic mass alone, though not completely, while adhering to the design of the SPARC photometric analysis of a constant mass to light ratio Υ_*, rather than a mass to light ratio that varies with the radial distance r as was implemented in our previous versions. Notably, there is still a dependence on the observed rotation curve velocities in that the coupling constant k depends on the final velocity v_f. Also, the coupling constant exponent β depends on the minimum error of the entire predicted-to-observed galaxy rotation velocities, as was implemented in this paper. In fact, only a single high quality data point on the velocity curve is required to get a value for β which makes a good fit, although we did not use this method here.

What we have presented here could possibly be used as an observing tool to gauge the outcome of the photometric observations of the stars in the disk and bulge of a galaxy as well as the radio observations of the HI gas density of the galaxy. We demonstrated in three out of the six galaxies presented above that a better fit can be made by minor adjustments to the disk, bulge or gas mass profiles. With the other three galaxies, no adjustments were made because the fits were deemed reasonable.

We believe that the GRST of dark matter in spiral and dwarf galaxies is a viable candidate for the unseen dark matter required to obtain the observed galaxy rotations. Since the gravitons make up the gravitational field, the graviton energy loss makes the field more negative, requiring more kinetic energy to attain a stable orbit. Gravitons themselves are already theorized by quantum gravity theories in their many forms [14]-[16]. In here, we utilize not the individual quantum but rather the bulk properties of gravitons just as is done for the cosmic microwave background radiation in the cosmos, which is a bulk behaviour of light. The fact that there is no generally acknowledged quantum theory of gravity does not prohibit the analysis of its macro physical aspects.

Finally, we showed how the GRST for galaxies can be fully incorporated into the general theory of relativity. This gives the GRST a greater measure of validity in describing galaxy dynamics.

7. Data Availability

The author declares that the data supporting the findings of this study are available within the paper, its supplementary information files, and from the SPARC website http://astroweb.cwru.edu/SPARC/.

Conflicts of Interest

The author declares no conflicts of interest regarding the publication of this paper.

References

[1] Oliveira, F.J. (2022) Theory of Gravitons in Spiral and Dwarf Galaxy Rotation Curves. *Journal of High Energy Physics, Gravitation and Cosmology*, **8**, 810-834. https://doi.org/10.4236/jhepgc.2022.83055

[2] Einstein, A. (1952) The Foundation of the General Theory of Relativity. Dover Publications, Inc.

[3] http://astroweb.cwru.edu/SPARC/

[4] Lelli, F., McGaugh, S.S. and Schombert, J.M. (2016) SPARC: Mass Models for 175 Disk Galaxies with Spitzer Photometry and Accurate Rotation Curves. *The Astronomical Journal*, **152**, 157-170. https://doi.org/10.3847/0004-6256/152/6/157

[5] McGaugh, S.S. (2005) The Baryonic Tully-Fisher Relation of Galaxies with Extended Rotation Curves and the Stellar Mass of Rotating Galaxies. *The Astrophysical Journal*, **632**, 859-871. https://doi.org/10.1086/432968

[6] Lelli, F., McGaugh, S.S. and Schombert, J.M. (2016) The Small Scatter of the Baryonic Tully-Fisher Relation. *The Astrophysical Journal Letters*, **816**, L14-L19. https://doi.org/10.3847/2041-8205/816/1/l14

[7] Schutz, B. (2022) A First Course in General Relativity. 3rd Edition, Cambridge University Press. https://doi.org/10.1017/9781108610865

[8] Misner, C.W., Thorne, K.S. and Wheeler, J.A. (1973) Gravitation. W.H. Freeman Princeton University Press.

[9] Deur, A. (2009) Implications of Graviton-Graviton Interaction to Dark Matter. *Physics Letters B*, **676**, 21-24. https://doi.org/10.1016/j.physletb.2009.04.060

[10] Sadun, A., Salmon, B., Evans, C. and Asadi-Zeydabadi, M. (2024) Dark Matter Den-

sity Profiles of Selected Spiral Galaxies. *International Journal of Astronomy and Astrophysics*, **14**, 172-183. https://doi.org/10.4236/ijaa.2024.143011

[11] Rothman, T. and Boughn, S. (2024) Can Gravitons Be Detected? https://arxiv.org/pdf/gr-qc/0601043

[12] Oliveira, F.J. (2022) How the Redshift of Gravitons Explains Dark Matter and Dark Energy. *Journal of Modern Physics*, **13**, 1348-1368. https://doi.org/10.4236/jmp.2022.1311084

[13] Oliveira, F.J. (2023) New Insights into the Action of Gravitons in Spiral Galaxies. *Journal of High Energy Physics*, *Gravitation and Cosmology*, **9**, 968-983.

[14] Rovelli, C., Weinberg, S.C., Landshoff, P. and Nelson, D.R. (2008) Quantum Gravity. Cambridge Monographs on Mathematical Physics. Cambridge University Press (Virtual Publishing).

[15] Zee, A. (2003) Quantum Field Theory in a Nutshell. Princeton University Press.

[16] Feynman, R.P., Morinigo, F.B., Wagner, W.G. and Hatfield, B. (1995) Feynman Lectures on Gravitation. Addison-Wesley.